



MRI evaluation of pediatric posterior fossa tumors and its correlation with histopathology: A prospective observational study

Anamika Shahi Satya Sundar Gajendra Mohapatra Supriya Sundar Mishra*

Department of Radiology, IMS & SUM Hospital, Siksha 'O' Anusandhan (Deemed to be) University, Bhubaneswar, Odisha, India.

ARTICLE INFO

Article history:

Received 8 July 2022

Accepted as revised 13 October 2022

Available online 2 November 2022

Keywords:

Posterior fossa, medulloblastoma, magnetic resonance imaging, MRI, pilocytic astrocytoma.

ABSTRACT

Background: The commonest malignancy in the pediatric age group is leukemia, followed by brain tumors. Pediatric brain tumors are usually seen in children below 10 years. The incidence ranges from 1 to 3 per 100,000 cases. Primary intracranial tumors most commonly occur in the posterior fossa in children while infratentorial tumors are predominant in children over 4 years. Infratentorial tumors are more common overall, accounting for 45-60% of all cases. Physiologic characteristics of the pediatric posterior fossa tumors are well represented in advanced MRI techniques, which results in better pre-operative tumor evaluation, and often better results.

Objectives: Primary intracranial tumors most commonly occur in the posterior fossa in children. Treatment and prognosis rely heavily on correct diagnosis. The most important modality for early diagnosis is MRI of the brain. This study aims to evaluate the role of MRI in pediatric posterior fossa tumors.

Materials and methods: Thirty-three patients in the pediatric age group (<18 years) with a clinical suspicion of posterior fossa tumors, referred to the department of Radiology for undergoing MRI of the brain with contrast were included in the study. These patients underwent surgery followed by histopathological examination (HPE). Five parameters from conventional MRI were chosen and correlated with histopathology (gold standard). Statistical analysis was done subsequently.

Results: Diffusion-weighted imaging (DWI) is the most accurate parameter (94%), followed by T2 weighted imaging (T2WI), gradient, and post-contrast sequence (91% each). Diffusion-weighted imaging and post-contrast sequence had the highest specificity (almost 96%) while DWI and T2WI had the highest sensitivity (90% each). All 5 parameters are useful in 85% of cases. Overall diagnostic accuracy of MRI was almost 94% compared to histopathology.

Conclusion: DWI is the best parameter, followed by T2WI, gradient imaging, and post-contrast sequence. MRI is highly accurate in the evaluation of pediatric posterior fossa tumors. In centers where advanced MRI techniques cannot be performed, some parameters from conventional MRI can be selected that aid in diagnosis. Our study shows that judicious use of 5 parameters can increase sensitivity, specificity, and diagnostic accuracy of MRI for pediatric posterior fossa tumors.

* Corresponding author.

Author's Address: Department of Radiology, IMS & SUM Hospital, Siksha 'O' Anusandhan (Deemed to be) University, Bhubaneswar, Odisha, India.

** E-mail address: supriyasundarmishra@gmail.com
doi: 10.12982/JAMS.2023.027
E-ISSN: 2539-6056

Introduction

The commonest malignancy in the pediatric age group is leukemia, followed by brain tumors.¹ Pediatric brain tumors are usually seen in children below 10 years.² The incidence ranges from 1 to 3 per 100,000 cases.^{3,4} Primary intracranial tumors most commonly occur in the posterior fossa in children.⁵ The location of the tumors is age dependent. In infants, supratentorial tumors are more common, while infratentorial tumors are predominant in children over 4 years. Infratentorial tumors are more common overall, accounting for 45-60% of all cases.^{6,7} The histological types in pediatric brain tumors vary widely, contrary to in adults. The commonest posterior fossa (infratentorial) tumors are medulloblastoma, pilocytic astrocytoma (juvenile), brainstem glioma, and ependymoma.^{1,3,7} Less common tumors include Atypical rhabdoid/teratoid tumor (ATRT), vestibular schwannoma, cerebellar gangliocytoma, dermoids, high-grade glioma, hemangioblastoma (HB), meningioma and metastatic lesions.³

Treatment and prognosis rely heavily on correct diagnosis. The clinical manifestations of posterior fossa tumors are gait disturbances, raised intracranial tension, and cranial nerve deficits, which depend on the location, size, and type of tumor.⁵ Tumors of the brainstem which are aggressive, manifest as signs of pyramidal tract defect and eye movement disorders. The evaluation is related to the symptoms at presentation. If the child is younger and unable to speak regarding his/her symptoms, then the evaluation is mostly based on clinical examination, achievement of milestones, response to stimuli, assessment of the nervous system, presence of symptoms such as diplopia, hearing loss, etc. On the other hand, if the child is relatively elder and able to speak about his symptoms, then the diagnosis is relatively easier compared to the younger group. The diagnosis proceeds to the intracranial space-occupying lesion (ICSOL) much earlier due to the elicitation of history by the patient. Subsequently, a clinical examination is done, similar to the one in the younger age group. Once the provisional diagnosis of a posterior fossa tumor is arrived at, the next line of management is a contrast-enhanced MRI of the brain, which is the investigation of choice.

Conventional sequences on MRI are useful in the evaluation of location, extent, type of tumor as well as areas of brain involvement (white or grey matter or both).³ Physiologic characteristics of the pediatric posterior fossa tumors are well represented in advanced MRI techniques, which results in better pre-operative tumor evaluation, and often better results. In centers where advanced MRI techniques cannot be performed due to cost/time factors or lack of technical expertise, often conventional MRI is the only modality of diagnosis. This study aims to evaluate the role of MRI in pediatric posterior fossa tumors and compare it with Histopathological examination (gold standard).

Materials and methods

This prospective, observational study was conducted in a tertiary care center, Department of Radiology, Institute of Medical Sciences (IMS), and SUM Hospital, Siksha 'O' Anusandhan (SOA) Deemed to be University, Bhubaneswar, Odisha, India. Informed consent was taken from all the patients

undergoing the study.

Selection and description of participants

We applied the following formula to calculate the sample size:

$$n = (Z)^2 * p * (1-p) / (d)^2$$

where

n = Sample Size

Z = Normal curve value for 99% Confidence (2.576)

p = Sensitivity of previous reference article (86.7%)

d = Absolute error or precision (20%)

Based on the sensitivity (86.7%) of MRI in the diagnosis of posterior fossa tumors with histopathology (gold standard) observed in an earlier publication by Ahmad T et al. and with 99% confidence and 20% allowable error, the sample size was calculated.⁸

Applying the formula to our study, the minimum sample size was 20. However, we were able to collect 33 patients for our study.

Study population

Our study population included all the patients who were referred to the Department of Radiodiagnosis with a clinical suspicion of posterior fossa tumors, for undergoing a pre-operative MRI of the brain.

Inclusion criteria

In our study, we included patients of the pediatric age group (aged 18 years or below), with a clinical suspicion of posterior fossa tumors, who underwent contrast-enhanced MRI of the brain.

Exclusion criteria

All patients who had undergone prior surgery for the posterior fossa tumors (post-operative cases) or posterior fossa masses of non-neoplastic etiology, were not included in our study.

Technical information

Conduct of the study

Pediatric patients (<18 years), with a clinical suspicion of posterior fossa tumors, were referred to the Department of Radiodiagnosis, for undergoing MRI of the brain with contrast. After obtaining informed consent, MRI was done in a 1.5 Tesla MRI system (General Electric Medical Systems, Milwaukee, WI, USA). Gadolinium-based contrast was administered at a dose of 0.1 mmol/kg.

Thirty-three patients in the pediatric age group underwent an MRI of the brain with contrast during the study period. Interpretation of MRI is generally done by at least 2 radiologists. One of them is a resident/trainee who prepares the provisional report and the other one is a faculty/consultant in the department, who has either an MD or DNB degree in Radiodiagnosis and finalizes the report. Very often a lot of MRIs with findings are discussed with 2-3 more faculties/consultants who share their experience and discuss similar cases seen in the past as a reference point.

Once these patients underwent surgical excision of the mass followed by histopathological examination (HPE) of the specimen, MRI findings were correlated with histopathology (gold standard), and relevant statistical analysis was done.

MRI parameters were chosen to aid in diagnosis

Five parameters were chosen from the MR imaging that was most helpful in arriving at a diagnosis. These included:

1. **Location of tumor:** Whether the tumor is located in the midline or off midline. Medulloblastoma, ependymoma, and brainstem glioma are the tumors that have a midline location while atypical teratoid/rhabdoid tumor (AT/RT), juvenile pilocytic astrocytoma and hemangioblastoma have a more common off midline location. So, on MRI, if a tumor had a midline location, it was assigned to be one of medulloblastoma, ependymoma, or brainstem glioma, depending on other parameters. While an off-midline location is expected to be one of atypical teratoid/rhabdoid tumor (AT/RT), juvenile pilocytic astrocytoma, and hemangioblastoma
2. **T2 signal:** Tumors can appear hypo, iso, or hyperintense to grey matter on the T2 sequence. Medulloblastoma appears isointense on T2 while the rest of the tumors are hyperintense. So, if a tumor appeared isointense on T2, it was assigned Medulloblastoma while hyperintensity meant it could be any of the other tumors.
3. **Diffusion imaging:** Tumors were classified according to whether they show restriction or no restriction on diffusion imaging. Medulloblastoma is the only tumor that shows diffusion restriction while the rest of the tumors do not. So, if diffusion restriction was seen, the tumor was assigned as Medulloblastoma. If no diffusion restriction, it could represent one of the other 4 tumors. Although teratoid/rhabdoid tumor (AT/RT) can show diffusion restriction, we did not have any MRI diagnosis of AT/RT.
4. **Gradient sequence:** Tumors were classified according to whether they show blooming on gradient sequence. Ependymoma is the only tumor that shows gradient blooming. So, if blooming on gradient sequence was seen, the tumor was assigned as ependymoma. If there was no gradient blooming, it could represent one of the other 4 tumors. Although teratoid/rhabdoid tumor (AT/RT) can show gradient blooming, we did not have any MRI diagnosis of AT/RT.
5. **Post contrast sequence:** Tumors were classified according to whether they show enhancement (homogenous or heterogeneous) or no enhancement on post-contrast sequences. Low-grade brainstem gliomas do not show post-contrast enhancement. So, if there was no post-contrast enhancement, the tumor was assigned as brainstem glioma. If there was enhancement (homogenous or heterogeneous), it could represent any of the other 5 tumors.

A diagnosis of a particular posterior fossa tumor was given if it satisfied at least 3 out of the 5 parameters.

Statistics

Statistical analysis was done using IBM SPSS version 22. Validity parameters namely sensitivity, specificity, accuracy, and positive/negative predictive values were computed for various MRI sequences concerning histopathology. Numerical variables were expressed as mean and standard deviations and the categorical variables were expressed as frequency and percentages. Chi-square test was used to test statistical significance. The value of $p<0.05$ was considered statistically significant.

Results

As seen in Figure 1, almost 73% of the tumors were located in the midline while the rest 27% had an off-midline location. Amongst the midline tumors, the most common were brainstem glioma and medulloblastoma (41% each) followed by ependymoma (17%). Amongst the off-midline tumors, pilocytic astrocytoma was most common (78%) followed by atypical teratoid/rhabdoid tumor and hemangioblastoma (11% each). The location of the tumor helped to provide a clue to the diagnosis in almost 94% of cases, while in 6% it was not helpful.

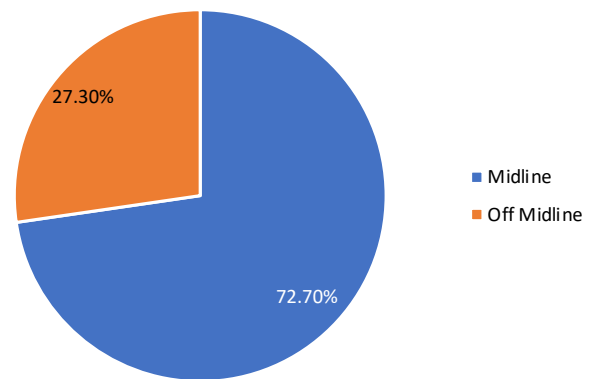


Figure 1. Pie chart of location of posterior fossa tumors (n=33).

One-third (33%) of the tumors were isointense on T2 weighted imaging while the rest two-thirds (66.67%) were hyperintense. As seen in Table 1, T2 weighted imaging had a sensitivity of 90% in predicting Medulloblastoma. Specificity was 91.30%, with a high negative predictive value of 95.45%. Overall diagnostic accuracy was 90.91%. Using the Chi-square test, a comparison of T2 weighted imaging and histopathology in diagnosing medulloblastoma was found to be statistically significant ($p<0.05$), as seen in Table 2.

In the gradient sequence, the majority of the tumors (almost 85%) did not show blooming, while only about 15% showed blooming. As seen in Table 3, the gradient sequence had a sensitivity of 75% in predicting the ependymoma. Specificity was 93.10%, with a high negative predictive

value was 96.43%, and the total diagnostic accuracy was 90.91%. Using the Chi-square test, a comparison of gradient sequence and histopathology in diagnosing ependymoma was found to be statistically significant ($p<0.05$), as seen in Table 4.

In our study, diffusion imaging showed restriction in about 30% of the patients. Rest 70% did not show diffusion restriction. As seen in Table 5, Diffusion imaging had a sensitivity of 90% in predicting medulloblastoma. Specificity was high at 95.65%, positive predictive value was 90%, negative predictive value was 95.65%, and total diagnostic accuracy was 93.94%. In our study, Diffusion imaging was helpful in diagnosis in almost 94% of patients. Diffusion-weighted imaging was the single most useful parameter in diagnosis. Using the Chi-square test, a comparison of diffusion-weighted imaging and histopathology in diagnosing medulloblastoma was found to be statistically significant ($p<0.05$), as seen in Table 6.

In post-contrast sequences, almost three-fourths of tumors (72.72%) showed enhancement and little over

one-fourth of tumors (27.27%) did not. As seen in Table 7, post contrast sequence had a sensitivity of 80% in predicting brainstem glioma. Specificity was high at 95.65%, and the total diagnostic accuracy was 90.91%. Using the Chi-square test, a comparison of post-contrast sequence and histopathology in diagnosing brainstem glioma was found to be statistically significant ($p<0.05$), as seen in Table 8.

As seen in Figure 2, In almost 85% of cases, all the parameters (sequences) were helpful in diagnosis. 4/5 of the parameters were helpful in 6% of cases. 3/5 and 2/5 parameters were useful in 3% of cases while none of the parameters were useful in about 3% of cases.

In our study, the overall accuracy of MRI in diagnosing pediatric posterior fossa tumors was almost 94% of patients. This is seen in Table 9.

Out of the total number of patients (33), the mean age in the study population was 6.6 years, ranging between 1 to 18 years. This is evident in Table 10.

Table 1 Validity parameters of T2 signal with histopathology in diagnosing medulloblastoma (n=33).

Parameter	Value (%)	95% CI	
		Lower	Upper
Sensitivity	90.00	55.50	99.75
Specificity	91.30	71.96	98.93
False positive rate	18.18	3.21	52.25
False negative rate	4.55	0.23	24.88
Positive predictive value	81.82	54.02	94.52
Negative predictive value	95.45	76.51	99.27
Diagnostic accuracy	90.91	75.67	98.08

Table 2 Comparison of T2 signal with histopathology in the diagnosis of medulloblastoma (n=33).

T2 Isointense	Medulloblastoma present (HPE diagnosis)		<i>p</i> value
	Yes	No	
Yes	9 (90%)	2 (8.7%)	<0.001
No	1 (10%)	21 (91.3%)	

Table 3 Validity parameters of gradient sequence with histopathology in diagnosing ependymoma (n=33).

Parameter	Value (%)	95% CI	
		Lower	Upper
Sensitivity	75.00	19.41	99.37
Specificity	93.10	77.23	99.15
False positive rate	40.00	7.25	82.95
False negative rate	3.57	0.18	20.23
Positive predictive value	60.00	25.99	86.50
Negative predictive value	96.43	83.14	99.33
Diagnostic accuracy	90.91	75.67	98.08

Table 4 Comparison of gradient sequence with histopathology in diagnosis of ependymoma (n=33).

Gradient blooming	Ependymoma present (HPE diagnosis)		<i>p</i> value
	Yes	No	
Yes	3 (75%)	2 (6.89%)	<0.001
No	1 (25%)	27 (93.10%)	

Table 5 Validity parameters of diffusion imaging in diagnosing medulloblastoma (n=33).

Parameter	Value (%)	95% CI	
		Lower	Upper
Sensitivity	90.00	55.50	99.75
Specificity	95.65	78.05	99.89
False positive rate	4.35	0.11	21.95
False negative rate	10.00	0.25	44.50
Positive predictive value	90.00	55.50	99.75
Negative predictive value	95.6	78.05	99.89
Diagnostic accuracy	93.94%	79.77	99.26

Table 6 Comparison of diffusion imaging with histopathology in diagnosis of medulloblastoma (n=33).

Diffusion Restriction on DWI	Medulloblastoma Present (HPE diagnosis)		<i>p</i> value
	Yes	No	
Yes	9 (90%)	1 (4.35%)	<0.001
No	1 (10%)	22 (95.65%)	

Table 7 Validity parameters of post contrast sequence in diagnosing brainstem glioma (n=33).

Parameter	Value (%)	95% CI	
		Lower	Upper
Sensitivity	80.00	44.39	97.48
Specificity	95.65	78.05	99.89
False positive rate	11.11	0.58	49.32
False negative rate	8.33	1.45	28.47
Positive predictive value	88.89	53.44	98.24
Negative predictive value	91.67	76.05	97.44
Diagnostic accuracy	90.91	75.67	98.08

Table 8 Comparison of post contrast sequence with histopathology in diagnosis of brainstem glioma (n=33).

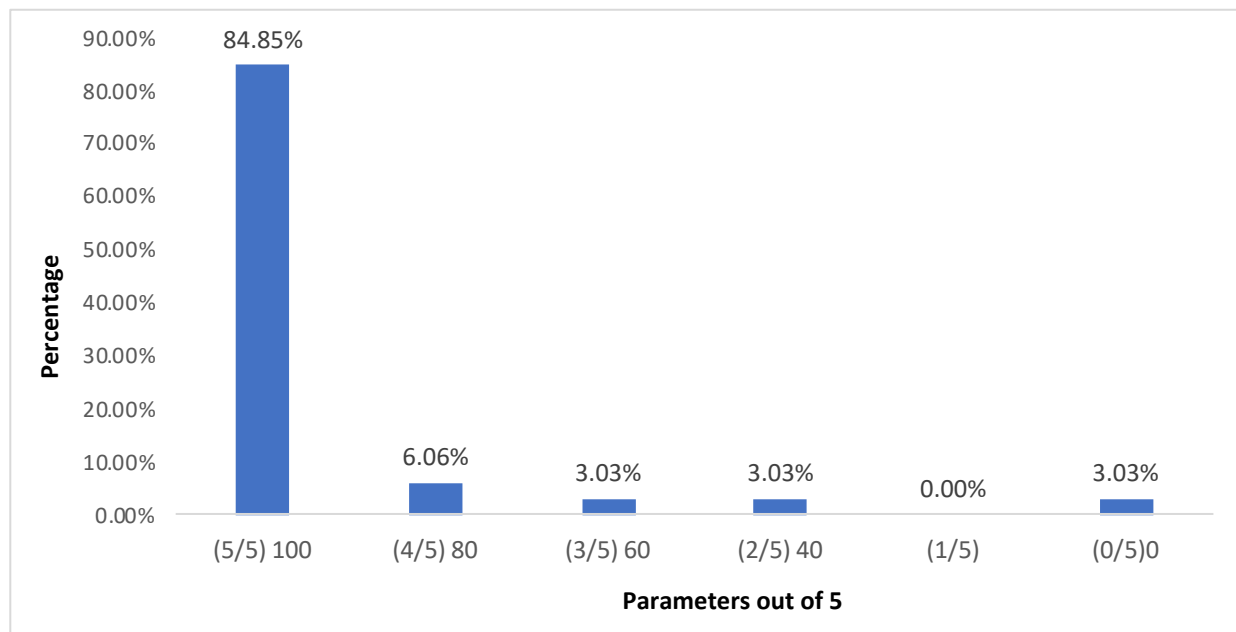
No post contrast Enhancement	Brainstem Glioma Present (HPE diagnosis)		<i>p</i> value
	Yes	No	
Yes	8 (80%)	1 (4.34%)	<0.001
No	2 (20%)	22 (95.65%)	

Table 9 MRI diagnosis correlating to histopathological diagnosis (gold standard) among the patients (n=33).

MRI correlates to HPE	Frequency	Percentage (%)
Yes	31	93.94
No	2	6.06

Table 10 Distribution of age among the patients (n=33).

Parameter	Mean \pm SD	Median	Min	Max
Age	6.64 \pm 4.34	6.00	1.00	18.00

**Figure 2.** MRI parameters helpful in diagnosis (out of 5) (n=33).

Discussion

In our study, the mean age of patients was 6.6 years. The range of age group was from 1 year to 18 years. According to Farwell *et al.*² the average age of onset is less than 10 years, which is seen in our study. There were slightly more males (51.5%) than females (48.5%) in our study, with a male-female ratio of 1.06:1. This is lesser than in the study by Farwell L *et al.*² where the ratio was 1.3:1, but slightly higher than the study by Yuh *et al.*⁹ where it was 1:1.

Almost three-fourths (72.7%) of the tumors were located in the midline. Brainstem glioma and medulloblastoma were the most common midline tumors (41.67% each). All brainstem gliomas and medulloblastomas were located in the midline, which is slightly more than the studies by Levy RA *et al.*¹⁰ and Poretti A *et al.* who observed that 75-90% of the medulloblastomas are located in the midline.³ In our study, all cases of ependymomas were located in the midline, which is similar to Plaza J *et al.*⁷ and Poretti A *et al.* who found that infratentorial ependymomas are located in the midline, on the floor of the fourth ventricle.³ Amongst the off-midline tumors, 78% were pilocytic astrocytomas, while rare tumors such as atypical teratoid/rhabdoid tumors and hemangioblastoma constituted 11% each. This is similar to findings by Jaremko JL *et al.*¹¹ who found that a tumor located off midline is most likely to be pilocytic astrocytoma, and Meyers SP *et al.*¹² where most atypical teratoid/rhabdoid tumors were located off midline. The location of the tumors provided a clue to the diagnosis in 93.90% of the cases.

Although Jaremko JL *et al.*¹¹ found that pilocytic astrocytoma was more likely to be off midline than medulloblastoma, they do not mention the full classification of tumors into midline or off midline and whether this parameter was used for diagnosis.

In T2 weighted imaging, almost one-third (30.30%) of the tumors were isointense, while the remaining 69.70% appeared hyperintense. Medulloblastomas are highly cellular and densely packed tumors, hence it is often T2 hypo to isointense compared to gray matter.^{3,7} Hence tumors appearing isointense on T2 weighted images were assigned as medulloblastomas, while hyperintense T2 signal meant one of the other tumors. In our study, if a lesion was isointense on T2 weighted images, it was highly indicative of medulloblastoma, while 90% of the patients with medulloblastoma had an isointense signal on T2WI (sensitivity of 90%). The absence of isointensity on T2WI (hyperintense signal on T2) almost excluded medulloblastoma (very high negative predictive value of 95.45%). Moreover, 91.30% of patients who did not have isointensity on T2 weighted imaging did not have medulloblastoma (specificity of 91.3%). This is similar to the studies by O'Brien WT¹ Poretti A *et al.*,³ Plaza J *et al.*,⁷ Meyers SP *et al.*,¹² and Koeller & Rushing who report that most of the medulloblastoma's have iso to hypointense signal on T2WI.¹³ The accuracy of T2 weighted imaging in diagnosing medulloblastoma was 90.91% compared to histopathology.

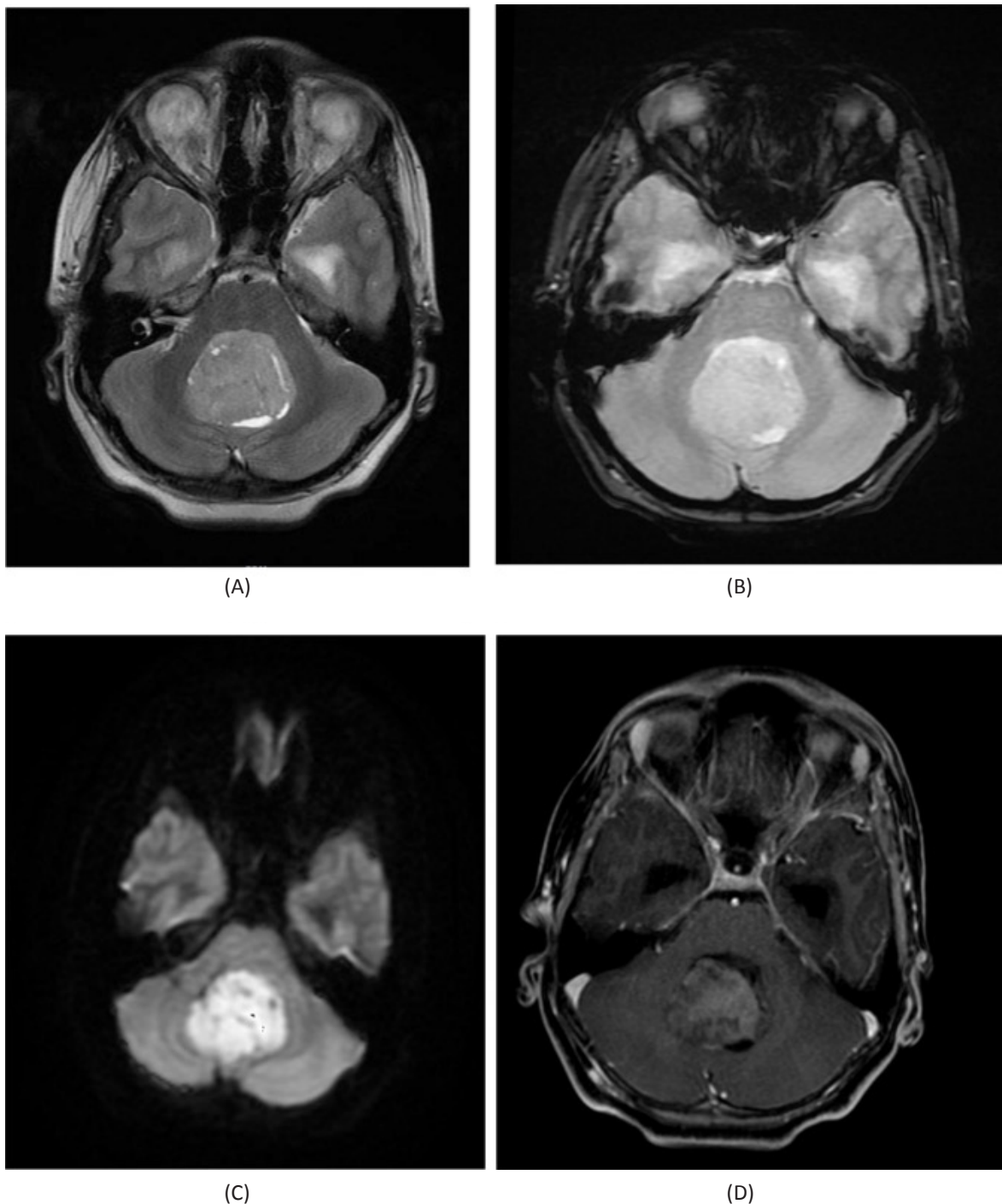


Image 1. Case of medulloblastoma. (A): axial T2 shows midline isointense mass, (B): axial SWAN sequence shows no blooming, (C): the mass appears bright on DWI (diffusion restriction), (D): post contrast sequence shows moderate enhancement.

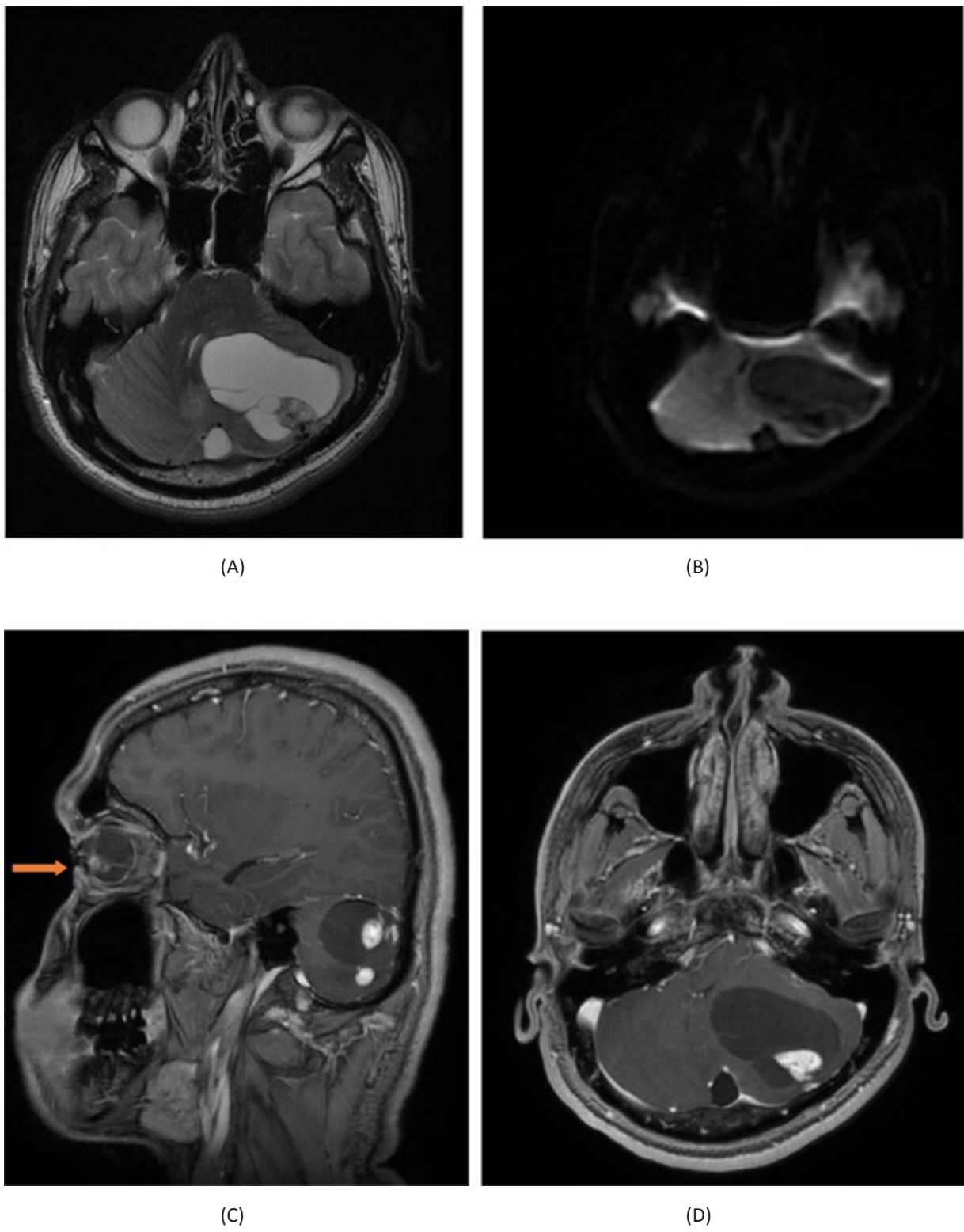


Image 2. Case of hemangioblastoma. (A): axial T2 shows left cerebellar (off midline) cystic mass with hyperintense nodules, (B): DWI shows no diffusion restriction, (C): left eye angioma (arrow), (D): post contrast sequence shows intense enhancement of the solid component. Patient was a known case of von Hippel-Lindau (VHL) syndrome..

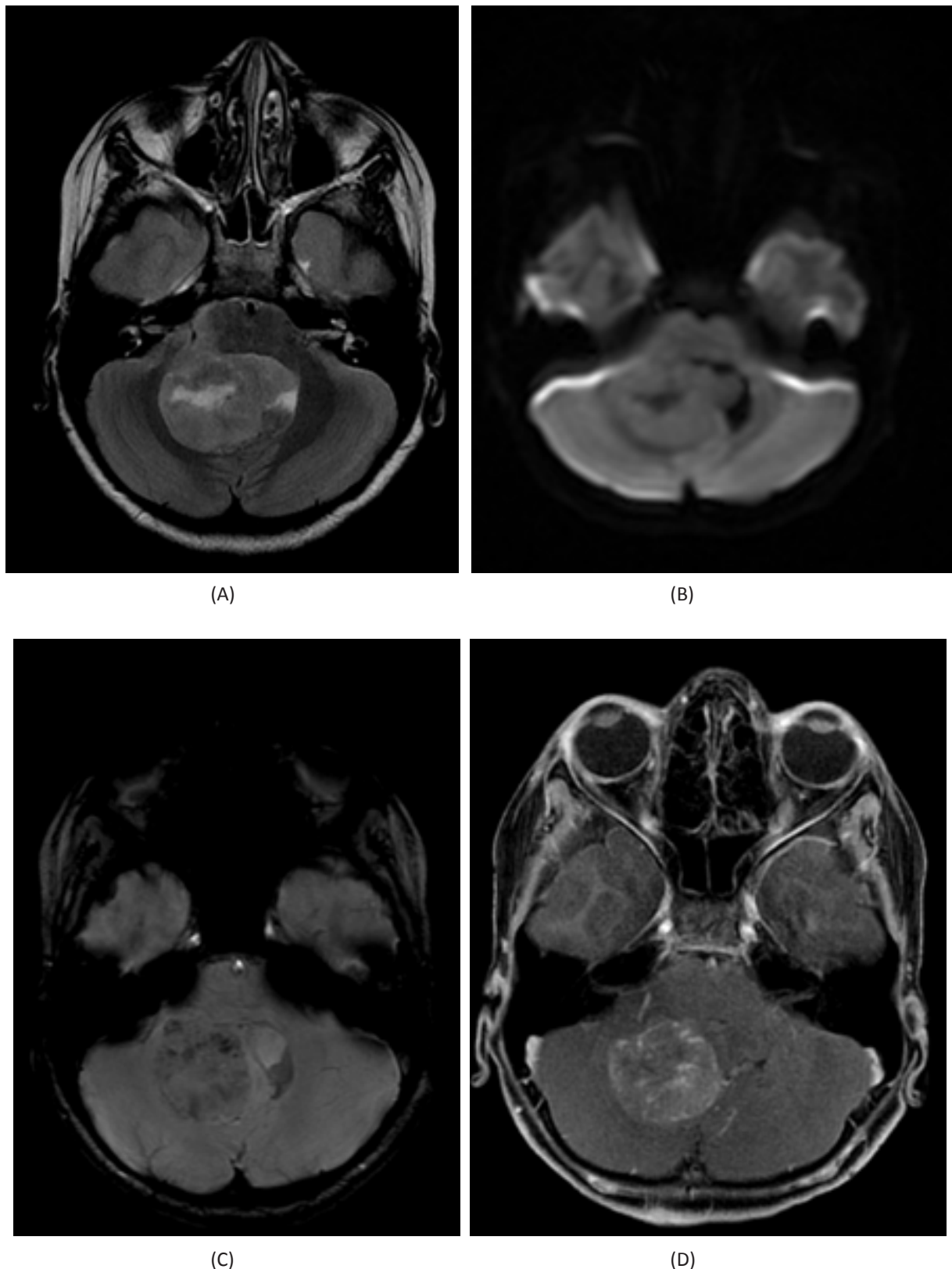


Image 3. Case of ependymoma. (A): axial T2 shows hyperintense midline mass, (B): DWI shows isointense mass (no diffusion restriction), (C): axial GRE sequence shows blooming, (D): post contrast sequence shows heterogenous enhancement.

Gradient imaging showed blooming in about 15.15% of tumors while the majority of the tumors (84.85%) showed no blooming. Plaza J et al.³ found that calcification is seen in half (50%) of ependymomas. Hemorrhage & calcification bloom on gradient sequences. Hence tumors that showed blooming on gradient sequences were assigned as ependymomas, while the ones that showed no blooming, could represent one of the other tumors. In our study, 75% of ependymoma cases showed gradient blooming (sensitivity of 75%), specificity was high at 93.10%, while the absence of gradient blooming almost excluded ependymoma (very high negative predictive value of 96.43%). The sensitivity is higher than the study by O'Brien WT where calcifications are seen in about half (50%) of the cases, cysts in about 20%, and hemorrhage in 10% (total 60% blooming), and Poretti A et al. who found calcifications in about half (50%) and old hemorrhages, which appear as focal hypointensities on all sequences of MRI.¹³ One of the differential diagnoses of medulloblastoma is ependymoma. In a study conducted by Koeller & Rushing it is seen that calcifications (which appear as blooming in gradient sequences) are typically seen in ependymomas, as opposed to medulloblastoma.¹² The diagnostic accuracy of gradient blooming in predicting ependymoma was 90.91%.

In our study, diffusion imaging showed that about 30% of tumors had restricted diffusion while the rest 70% showed no restriction. Koeller & Rushing found that medulloblastoma typically shows restricted diffusion on diffusion-weighted imaging (DWI).¹² Hence tumors that showed diffusion restriction were assigned as Medulloblastomas, while the ones that showed no restricted diffusion could represent one of the other tumors. In our study, diffusion imaging was very highly specific (95.65%) and sensitive (90%) for medulloblastoma. While the absence of diffusion restriction almost excluded medulloblastoma (very high negative predictive value of 95.65%). Our study had higher specificity than the study by Forbes et al. where the sensitivity and specificity of diffusion imaging in diagnosing medulloblastoma were 94% each, however, our sensitivity was slightly lower at 90%.¹⁴ Our specificity was slightly lower than Camacho CA et al. who report that an apparent diffusion coefficient value of $<0.9 \times 10^{-3}$ mm²/sec is found to be 100% specific in differentiating medulloblastoma from astrocytoma and ependymoma.¹⁵ Medulloblastoma typically shows restricted diffusion on DWI and lower values on apparent diffusion coefficient (ADC). This allows differentiation from ependymoma, pilocytic astrocytoma, and brainstem gliomas, as observed by Poretti A et al. and Plaza J et al.^{3,7} Aquilina K found that high cellular density in medulloblastoma is seen as diffusion restriction on DWI. Jaremko JL et al. observed that in Ependymoma and Pilocytic Astrocytoma, the ADC values are higher than in medulloblastoma, and DWI-ADC is very useful to differentiate tumors of the posterior fossa in children.¹¹ Poretti et al. found that the ADC values of posterior fossa tumors in the pediatric age group can help differentiate the different types of tumors and predict their histological grades.³ In our study, diffusion imaging had the highest diagnostic accuracy amongst all the parameters, at almost 94%, and hence was the single best parameter for

diagnosis of posterior fossa tumors.

In post-contrast sequences, almost three-fourths of tumors (72.72%) showed enhancement, out of which 33.33% showed homogenous enhancement while 39.39% showed heterogeneous enhancement. Little over one-fourth of tumors (27.27%) showed no enhancement. Plaza J et al. report that most of the gliomas in the brainstem show no enhancement on MRI, and enhancement, is heterogeneous if it is seen in some cases.⁷ Hence, any tumor that did not show post-contrast enhancement was assigned as glioma while if there was enhancement (homogenous or heterogeneous) could represent one of the other tumors. In our study, 95.65% of patients who did not have post-contrast enhancement did not have glioma, thus giving a very high specificity of 95.65%, while sensitivity was 80%. The presence of enhancement almost excluded brainstem glioma (high negative predictive value of 91.67%). This is similar to Poretti L et al.³ who observed that enhancement in post-contrast sequences is variable, but most brainstem gliomas elicit minimal or no post-contrast enhancement. Camacho CA et al.¹⁵ found that most of the gliomas of the brainstem do not show uniform enhancement. If there is some enhancement, the enhancing portion correlates to higher grades of the tumor. This is the reason for slightly lower sensitivity (80%) in our study as the 20% of tumors showing some enhancement (false negative) turned out to be medium or high grade. Aquilina K report that brainstem gliomas generally show no enhancement on post-contrast imaging.⁵ The diagnostic accuracy of post-contrast enhancement MRI in predicting brain stem glioma was 90.91%.

All five MRI parameters namely, location of the tumors, iso-intensity on T2, gradient blooming, diffusion restriction, and post-contrast sequence taken together, were accurate in diagnosing almost 85% of the cases of posterior fossa tumors.

In our study, there were 31/33 cases were diagnosed accurately by MRI. Hence the overall diagnostic accuracy of MRI to histopathological examination (gold standard) was very high, at almost 94% (93.94% to be precise). This is slightly higher than the study by Forbes et al. who reported the predictive accuracy of MRI ranged from 78% to 93%.¹⁴

There were two cases whose MRI diagnosis did not correlate with histopathology. In the 1st case, the lesion was located in the pons (brainstem), was T2 hyperintense, no diffusion restriction or gradient blooming. No post-contrast enhancement was seen. MRI features were suggestive of low-grade glioma. As the tumor was growing rapidly in size, the biopsy was taken, which turned out to be grade IV medulloblastoma (PNET). None of the imaging features were suggestive of medulloblastoma. The patient later expired.

The 2nd case was predominantly a solid mass with cystic areas in the periphery and epicenter at the fourth ventricle. It was infiltrating the right cerebellar hemisphere, vermis, pons, and medulla with obstructive hydrocephalus.

On MRI sequences, it was hyperintense on T2, showed diffusion restriction and gradient blooming, and mild patchy post-contrast enhancement was seen. A provisional diagnosis of ependymoma was given. Histopathology was suggestive of atypical teratoid-rhabdoid tumor (AT/RT), which was later sent for IHC, which showed loss of INI-1, thus confirming the diagnosis. As AT/RT is a very rare posterior fossa tumor^{3,7,12,16} it is very difficult to give it as a pre-operative diagnosis, based on just imaging findings. This patient too expired.

The differentiation of hemangioblastoma from pilocytic astrocytoma is challenging on conventional MRI. Hemangioblastoma and PA have overlapping imaging features. Subtle differences in the conventional MR imaging of hemangioblastomas are helpful in diagnosis such as extensive flow voids in and around the tumor, the mural nodule abutting the pial surface, and hemorrhage in about 20-25% of cases.¹⁷ Further advanced MRI techniques such as increased perfusion and lower NAA/Cr values in MR spectroscopy aid the diagnosis. Clinically, association with von Hippel-Lindau (VHL) syndrome (44-72%) and higher age (hemangioblastoma is rare in children <18 years old) give a clue to the diagnosis. In our study, the patient was an 18-year-old child and a known case of von Hippel-Lindau (VHL) syndrome and had a large cystic lesion (T2 hyperintense) with peripherally enhancing nodules. There were few flow voids at the periphery of the lesion. No diffusion restriction or gradient blooming was seen while the nodules showed intense heterogeneous post-contrast enhancement. It is difficult to differentiate hemangioblastoma from pilocytic astrocytoma by just using the parameters chosen in our study. However, the overall morphology of the tumor, age, and clinical association of von Hippel-Lindau (VHL) syndrome aided the diagnosis. In such cases, advanced MRI techniques should be used, such as perfusion imaging (which will show increased perfusion) and MR spectroscopy (which will show lower NAA/Cr values) will help clinch the diagnosis.

There have been multiple studies on the role of MRI in pediatric posterior fossa tumors. But we did not find any study done previously, where specific sequences (parameters) chosen from the conventional MRI sequences were useful in predicting the diagnosis of tumors, especially where multiple individual parameters helped in diagnosis (like T2 helpful in the diagnosis of medulloblastoma, gradient for ependymoma, diffusion imaging for medulloblastoma and post-contrast sequence for brainstem gliomas). We selected sequences from the conventional MRI and used them to diagnose a particular tumor. In none of the previous studies, we found this kind of methodology, where single MRI sequences were useful in the diagnosis of a tumor. There were multiple such parameters chosen, each one helping in the diagnosis of a particular tumor. Hence, taken together, they help arrive at a diagnosis, which was highly predictive of the tumor, for histopathology (which is the gold standard for diagnosis).

With the results of our study, we searched for articles with a similar topic. From a lot of reference articles, we found that our results (usefulness of MRI in the diagnosis of pediatric posterior fossa tumors concerning histopathology,

which is the gold standard) were comparable to previous studies, with most results better than others while the rest being at par. With such results comparable to standard reference published articles, we felt that our study is worth publishing too, as it provides something new, which is not seen in previous articles (multiple single parameters chosen from routine MRI sequences helpful in the diagnosis of multiple posterior fossa tumors). Moreover, there is no additional cost or time spent by the patient. The study population included cases that were sent to our department for MRI (who fulfilled the inclusion criteria). An accurate diagnosis can arrive fairly quickly as we used only the routine MRI sequences, that the patients were already about to undergo. This is vital in cases that require urgent surgical interventions. As proven in our study, since conventional MRI is highly accurate in diagnosing pediatric posterior fossa tumors, these patients can be taken up for emergency surgeries, right out of the MRI room (the report is usually prepared while the scan is going on, especially in emergency cases).

Conclusion

Diffusion-weighted imaging is the single best parameter helpful in the diagnosis of pediatric posterior fossa tumors (accuracy of almost 94%). It was followed by T2 weighted imaging, gradient imaging, and post-contrast sequence, all of which had accuracy of almost 91%. Together, all 5 parameters are useful in the diagnosis of 85% of cases. The overall accuracy of MRI in diagnosing pediatric posterior fossa tumors was very high at almost 94% for histopathological examination (gold standard).

References

- [1] O'Brien WT. Imaging of primary posterior fossa brain tumors in children. *J Am Osteopath Coll Radiol*. 2013; 11; 2(3): 2-12.
- [2] Farwell JR, Dohrmann GJ, Flannery JT. Central nervous system tumors in children cns tumors in children. *Cancer*. 1977; 40(6): 3123-32.
- [3] Poretti A, Meoded A, Huisman TA. Neuroimaging of pediatric posterior fossa tumors including review of the literature. *J Magn Reson Imaging*. 2012; 35(1): 32-47.
- [4] Baldwin RT, Preston-Martin S. Epidemiology of brain tumors in childhood—a review. *Toxicol appl Pharmacol*. 2004; 199(2): 118-31.
- [5] Aquilina K. Posterior fossa tumors in children – an overview of diagnosis and management. *Adv Clin Neurosci Rehabil*. 2013; 13(4): 24-8.
- [6] Pollack IF. Brain tumors in children. *N Engl J Med*. 1994; 331(22): 1500-7.
- [7] Plaza MJ, Borja MJ, Altman N, Saigal G. Conventional and advanced MRI features of pediatric intracranial tumors: posterior fossa and suprasellar tumors. *Am J Roentgenol*. 2013; 200(5): 1115-24.
- [8] Ahmad T, Gohar M. MRI evaluation of medulloblastoma with histopathological correlation. *Biomedica*. 2014; 30(3) : 1.
- [9] Yuh EL, Barkovich AJ, Gupta N. Imaging of ependymomas: MRI and CT. *Child's Nerv Syst*. 2009; 25(10): 1203-13.
- [10] Levy RA, Blaivas M, Muraszko K, Robertson PL. Desmoplastic medulloblastoma: MR findings. *Am J Neuroradiol*. 1997; 18(7): 1364-6.
- [11] Jaremko JL, Jans LB, Coleman LT, Ditchfield MR. Value and limitations of diffusion-weighted imaging in grading and diagnosis of pediatric posterior fossa tumors. *Am J Neuroradiology*. 2010; 31(9): 1613-6.
- [12] Meyers SP, Khademian ZP, Biegel JA, Chuang SH, Korones DN, Zimmerman RA. Primary intracranial atypical teratoid/rhabdoid tumors of infancy and childhood: MRI features and patient outcomes. *Am J Neuroradiol*. 2006; 27(5): 962-71.
- [13] Koeller KK, Rushing EJ. From the archives of the AFIP: medulloblastoma: a comprehensive review with radiologic-pathologic correlation. *Radiographics*. 2003; 23(6): 1613-37.
- [14] Forbes JA, Reig AS, Smith JG, Jermakowicz W, Tomycz L, Shay SD, Sun DA, Wushensky CA, Pearson MM. Findings on preoperative brain MRI predict histopathology in children with cerebellar neoplasms. *Pediatr Neurosurg*. 2011; 47(1): 51-9.
- [15] Camacho AC, Chaljub G, Uribe T, Patterson JT, Swischuk LE. MR Imaging of Pediatric Posterior Fossa Tumors; *Contemp Diagn Radiol* 2017; 30(14): 1-6.
- [16] Louis DN, Ohgaki H, Wiestler OD, Cavenee WK, Burger PC, Jouvet A, Scheithauer BW, Kleihues P. The 2007 WHO classification of tumors of the central nervous system. *Acta Neuropathol*. 2007; 114(2): 97-109.
- [17] Lee SR, Sanches J, Mark AS, Dillon WP, Norman D, Newton TH. Posterior fossa hemangioblastomas: MR imaging. *Radiology*. 1989; 171(2): 463-8.